Inorganic Chemistry
Article

Inorg. Chem. **2010**, *49*, 5157–5166 **5157**
DOI: 10.1021/ic100290j

Synthesis, Characterization, and Structures of Uranium(III) *N,N*-Dimethylaminodiboranates

Scott R. Daly and Gregory S. Girolami*

The School of Chemical Sciences, University of Illinois at Urbana−Champaign, 600 South Mathews Avenue, Urbana, Illinois 61801

Received February 11, 2010

The reaction of UCl_4 with sodium *N,N*-dimethylaminodiboranate, $Na(H_3BNMe_2BH_3)$, in diethyl ether affords the uranium(III) product $U(H_3BNMe_2BH_3)_3$, which has been crystallized as two different structural isomers from pentane and toluene, respectively. The isomer crystallized from pentane is a polymer in which each uranium center is bonded to three chelating $H_3BNMe_2BH_3^-$ (DMADB) ligands and to one hydrogen atom from a neighboring molecule so as to form an intermolecular B−H−U bridge; each uranium center is coordinated to 13 hydrogen atoms. The isomer crystallized from toluene is also polymeric, but the uranium atoms are coordinated by two chelating DMADB ligands and two bridging DMADB ligands bound in a U(κ^3*H*-$H_3BNMe_2BH_3$-κ^3*H*)U fashion, so that each uranium atom is 14-coordinate. When the reaction of UCl_4 with $Na(H_3BNMe_2BH_3)$ is conducted in tetrahydrofuran (thf) or 1,2-dimethoxyethane (dme), the adducts $U(H_3BNMe_2BH_3)_3$(thf) and $U(H_3BNMe_2BH_3)_3$(dme) are obtained. The rate of reduction from U^{IV} to U^{III} is correlated with the donor ability of the solvent, the relative rates being Et_2O > thf > dme. The addition of trimethylphosphine to $U(H_3BNMe_2BH_3)_3$(thf) generates $U(H_3BNMe_2BH_3)_3(PMe_3)_2$. This compound slowly decomposes at room temperature over several months to yield the new borane $PMe_3BH_2NMe_2BH_3$, μ-(*N,N*-dimethylamido)pentahydro(trimethylphosphine)diboron. Single crystal X-ray diffraction studies, ^1H and ^{11}B NMR spectra, IR data, and field ionization mass spectra for the uranium complexes are reported.

Introduction

Actinide borohydride complexes are an intriguing class of metal complexes with fascinating structures and unusual properties.[1,2] Their inner coordination spheres consist largely or entirely of hydrogen atoms, their coordination numbers are high (often 12 or greater), and many are highly volatile; for example, $U(BH_4)_4$ sublimes readily at room temperature and has a vapor pressure of 4 Torr at 60 °C.[3] The high volatility of this latter complex (and its methylborohydride analogue) made it a candidate for enriching uranium in the ^{235}U isotope by gaseous diffusion during the Manhattan project. Ultimately, UF_6 became the material of choice for this purpose: although it is highly corrosive, this problem could be (and was) solved. Using $U(BH_4)_4$ in the gaseous diffusion process would have been less practical because it decomposes rapidly above 100 °C (thus limiting the amount of material that can be put into the vapor phase) and because the ^{10}B and ^{11}B isotopes would have to be separated in a previous step.

Complexes of stoichiometry $M(BH_4)_4$ are known for five of the actinide elements (Th−Pu).[4−6] Crystallographic studies show that $M(BH_4)_4$ complexes of actinides with larger radii, thorium, protactinium, and uranium, adopt three-dimensional polymeric structures in the solid state in which the metal centers are 14 coordinate. Each metal center is bound to two κ^3-BH_4^- ligands and four κ^2-BH_4^- ligands;[7] the latter bridge between metal centers in a κ^2,κ^2 fashion.[8,9] These compounds are volatile because the polymers readily depolymerize to form $M(BH_4)_4$ monomers in which all four BH_4^- ligands are κ^3.[10] In contrast, actinides with smaller radii, neptunium and plutonium, form $M(BH_4)_4$ complexes

*To whom correspondence should be addressed. E-mail: ggirolam@uiuc.edu.

(1) Ephritikhine, M. *Chem. Rev.* **1997**, *97*, 2193–2242.
(2) Makhaev, V. D. *Russ. Chem. Rev.* **2000**, *69*, 727–746.
(3) Schlesinger, H. I.; Brown, H. C. *J. Am. Chem. Soc.* **1953**, *75*, 219–221.
(4) Hoekstra, H. R.; Katz, J. J. *J. Am. Chem. Soc.* **1949**, *71*, 2488–2492.
(5) Ehemann, M.; Nöth, H. *Z. Anorg. Allg. Chem.* **1971**, *386*, 87–101.
(6) Banks, R. H.; Edelstein, N. M.; Rietz, R. R.; Templeton, D. H.; Zalkin, A. *J. Am. Chem. Soc.* **1978**, *100*, 1957–1958.
(7) We employ here a sensible but non-standard version of the kappa nomenclature, using it as a prefix and omitting as unnecessary the descriptor that indicates which kind of atom bridges to the metal center. See *Nomenclature of Inorganic Chemistry, IUPAC Recommendations 2005*; Connelly, N. G., Damhus, T., Hartshorn, R. M., Hutton, A. T., Eds.; RSC Publishing: Cambridge, 2005; Section IR-9.2.4.2.
(8) Bernstein, E. R.; Hamilton, W. C.; Keiderling, T. A.; La Placa, S. J.; Lippard, S. J.; Mayerle, J. J. *Inorg. Chem.* **1972**, *11*, 3009–3016.
(9) Charpin, P.; Nierlich, M.; Vigner, D.; Lance, M.; Baudry, D. *Acta Crystallogr., Sect. C: Cryst. Struct. Commun.* **1987**, *C43*, 1465–1467.
(10) Haaland, A.; Shorokhov, D. J.; Tutukin, A. V.; Volden, H. V.; Swang, O.; McGrady, G. S.; Kaltsoyannis, N.; Downs, A. J.; Tang, C. Y.; Turner, J. F. *Inorg. Chem.* **2002**, *41*, 6646–6655.

Published on Web 05/07/2010

that adopt 12-coordinate monomeric structures with four κ^3-BH_4^- ligands even in the condensed state.[6,11] These monomers are liquids at room temperature, and are more volatile than their polymeric Th, Pa, and U cousins.

The volatility of Th, Np, and U borohydride complexes can be increased by preventing polymerization in the solid-state. One way to accomplish this desideratum is to employ the monomethylborohydride ligand, BH_3Me^-, whose methyl substituent is a poor bridging group.[12,13] These resulting monomeric $M(\kappa^3\text{-}BH_3Me)_4$ complexes of Th and U are much more volatile than their polymeric BH_4^- analogues. For example, $Th(BH_3Me)_4$ sublimes in vacuum at 50 °C, compared to at 120 °C for $Th(BH_4)_4$. Another strategy to prevent polymerization in the solid state is to employ mixed ligand sets, which combine borohydride with other ligands.[14,15]

We have recently been exploring a new class of metal borohydride complexes based on the *N*,*N*-dimethylaminodiboranate anion, $H_3BNMe_2BH_3^-$ (DMADB).[16,17]

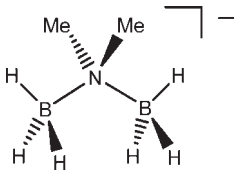

The DMADB anion, which consists of two BH_3 groups joined by an amido linker, is able to chelate to metals by means of four B−H−M bridges. Relative to BH_4^-, it occupies more space in the coordination sphere of a metal center and therefore is better able to inhibit polymerization that can reduce volatility. As a result, some DMADB complexes have proven to be highly volatile. For example, $Mg(H_3BNMe_2BH_3)_2$ is more volatile than any other magnesium compound reported to date: it sublimes at room temperature at 10^{-2} Torr (P_{vap} = 800 mTorr at 25 °C),[18] versus a sublimation temperature of 230 °C at 10^{-2} Torr for $Mg(BH_4)_2$.[19] Similarly, DMADB complexes of the lanthanides are some of the most volatile compounds of these metals ever prepared.[20]

Here we describe an extension of our efforts to the chemistry of the actinide element, uranium. Portions of this work have been described in a preliminary communication.[21]

Results and Discussion

Synthesis and Characterization of $U(H_3BNMe_2BH_3)_3$. The reaction of UCl_4 with 4 equiv of sodium *N*,*N*-dimethylaminodiboranate, $Na(H_3BNMe_2BH_3)$ in Et_2O initially gives a green solution that turns brown within a few hours with evolution of gas. As we will show below, the color change is probably associated with reduction of U^{IV} to U^{III}, with concomitant formation of H_2. Evaporation of the reaction mixture, followed by extraction of the residue into pentane, affords a light brown solution from which crystals of the uranium(III) complex $U(H_3BNMe_2BH_3)_3$, **1a**, may be obtained. The yield of product is low owing to the low solubility of **1a** in pentane (however, see below).

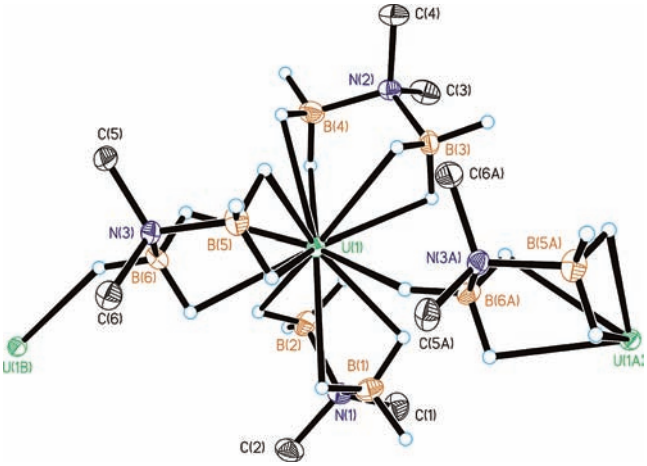

Figure 1. Molecular structure of $U(H_3BNMe_2BH_3)_3$, **1a**, obtained from pentane. Ellipsoids are drawn at the 35% probability level, except for hydrogen atoms, which are represented as arbitrarily sized spheres. The hydrogen atoms on the methyl groups have been removed for clarity.

The X-ray crystal structure of **1a** reveals that each uranium center is coordinated to three chelating $H_3BNMe_2BH_3$ ligands arranged in a propeller-like conformation (Figure 1; Table 2). Two hydrogen atoms on each of the six BH_3 groups bridge to the uranium center; the average of these twelve U−H distances is 2.49 Å. The U···B distances are 2.842(6)−2.935(6) Å, and the B−N−B angles within the ligands are 108.8(4)−109.8(4)°. Interestingly, the uranium atom is displaced 0.30 Å out of the plane defined by the three nitrogen atoms, along the axis of the pseudo 3-fold rotational symmetry element. The U^{III} complexes $U[N(SiMe_3)_2]_3$ and $U[CH(SiMe_3)_2]_3$ also lie 0.46 Å and 0.90 Å out of the plane of the three nitrogen or carbon atoms, respectively,[22,23] but there is a significant difference. The latter two complexes are monomers in the solid state, but in **1a** the displacement is due to formation of an intermolecular U−H interaction with a hydrogen atom from an adjacent molecule. The extra intermolecular U−H bond, which is coincident with the pseudo 3-fold rotation axis, makes the total coordination number of each uranium center 13, and links the uranium atoms into a chain so that the structure is in fact a linear polymer. The intermolecular U−H distance of 2.50 Å falls into the middle of the 2.37−2.60 Å range observed for the 12 U−H distances of the chelating DMADB ligands. The U···U distance between adjacent uranium centers in the chain is 5.991(6) Å.

The poor solubility of **1a** in pentane and other alkanes led us to investigate toluene as a solvent to extract the crude residue from the reaction of UCl_4 and

(11) Banks, R. H.; Edelstein, N. M.; Spencer, B.; Templeton, D. H.; Zalkin, A. *J. Am. Chem. Soc.* **1980**, *102*, 620–623.
(12) Schlesinger, H. I.; Brown, H. C.; Horvitz, L.; Bond, A. C.; Tuck, L. D.; Walker, A. O. *J. Am. Chem. Soc.* **1953**, *75*, 222–224.
(13) Shinomoto, R.; Gamp, E.; Edelstein, N. M.; Templeton, D. H.; Zalkin, A. *Inorg. Chem.* **1983**, *22*, 2351–2355.
(14) Baudry, D.; Charpin, P.; Ephritikhine, M.; Folcher, G.; Lambard, J.; Lance, M.; Nierlich, M.; Vigner, J. *J. Chem. Soc., Chem. Commun.* **1985**, 1553–1554.
(15) Scott, P.; Hitchcock, P. B. *J. Chem. Soc., Dalton Trans.* **1995**, 603–609.
(16) Keller, P. C. *Inorg. Chem.* **1971**, *10*, 2256–2259.
(17) Nöth, H.; Thomas, S. *Eur. J. Inorg. Chem.* **1999**, 1373–1379.
(18) Kim, D. Y.; Girolami, G. S. *Inorg. Chem.* **2010**, in press.
(19) Plesek, J.; Hermanek, S. *Collect. Czech. Chem. Commun.* **1966**, *31*, 3845–3858.
(20) Daly, S. R.; Kim, D. Y.; Yang, Y.; Abelson, J. R.; Girolami, G. S. *J. Am. Chem. Soc.* **2010**, *132*, 2106–2107.
(21) Daly, S. R.; Girolami, G. S. *Chem. Commun.* **2010**, *46*, 407–408.
(22) Van der Sluys, W. G.; Burns, C. J.; Sattelberger, A. P. *Organometallics* **1989**, *8*, 855–857.
(23) Stewart, J. L.; Andersen, R. A. *Polyhedron* **1998**, *17*, 953–958.

Table 1. Crystallographic Data for $U(H_3BNMe_2BH_3)_3$ Structural Isomers **1a** and **1b**, $U(H_3BNMe_2BH_3)_3(thf)$, **2**, $U(H_3BNMe_2BH_3)_3(PMe_3)_2$, **4**, and $PMe_3BH_2NMe_2BH_3$, **5**, at 193 K

	1a	**1b**	**2**	**4**	**5**
formula	$C_6H_{36}B_6N_3U$	$C_6H_{36}B_6N_3U$	$C_{10}H_{44}B_6N_3OU$	$C_{12}H_{54}B_6N_3P_2U$	$C_5H_{20}B_2NP$
FW (g mol^{-1})	453.27	453.27	525.37	605.41	146.81
λ (Å)	0.71073	0.71073	0.71073	0.71073	0.71073
crystal system	monoclinic	monoclinic	cubic	orthorhombic	orthorhombic
space group	$P2_1/c$	$P2_1/c$	$I23$	$Pbca$	$Pca2_1$
a (Å)	15.9392(4)	12.3571(6)	16.6987(2)	16.7492(12)	15.3721(13)
b (Å)	10.2456(3)	10.8128(6)	16.6987(2)	10.4449(7)	6.6323(5)
c (Å)	11.4154(3)	14.6145(7)	16.6987(2)	33.515(3)	10.1018(9)
β(deg)	97.192(1)	96.116(3)	90	90	90
V (Å^3)	1849.54(9)	1941.6(2)	4656.4(1)	5863.2(7)	1029.90(19)
Z	4	4	8	8	4
ρ_{calc} (g cm^{-3})	1.628	1.551	1.499	1.372	0.947
μ (mm^{-1})	8.757	8.342	6.971	5.647	0.199
R(int)	0.1043	0.0910	0.0600	0.0726	0.0523
abs corr method	face-indexed	face-indexed	face-indexed	face-indexed	face-indexed
max., min transm. factors	0.843, 0.190	0.754, 0.456	0.306, 0.162	0.799, 0.272	0.992, 0.941
data/restraints/params	4251/0/151	5035/49/223	1799/5/90	6684/0/229	1980/5/108
GOF on F^2	0.925	0.904	1.024	1.010	0.950
R_1 [$I > 2\sigma(I)$][a]	0.0318	0.0345	0.0144	0.0234	0.0346
wR_2 (all data)[b]	0.0701	0.0776	0.0332	0.0512	0.0771
max, min $\Delta\rho_{electron}$ (e·Å^{-3})	2.905/−2.556	4.175/−1.927	0.580/−0.351	0.754/−0.756	0.195/−0.152

[a] $R_1 = \sum||F_o| - |F_c||/\sum|F_o|$ for reflections with $F_o^2 > 2\,\sigma(F_o^2)$. [b] $wR_2 = [\sum w(F_o^2 - F_c^2)^2/\sum w(F_o^2)^2]^{1/2}$ for all reflections.

Table 2. Selected Bond Lengths and Angles for $U(H_3BNMe_2BH_3)_3$, **1a**[a]

Bond Lengths (Å)			
U(1)−B(1)	2.857(6)	U(1)−H(3D)	2.46
U(1)−B(2)	2.863(6)	U(1)−H(3E)	2.44
U(1)−B(3)	2.842(6)	U(1)−H(4D)	2.50
U(1)−B(4)	2.915(7)	U(1)−H(4E)	2.56
U(1)−B(5)	2.897(6)	U(1)−H(5D)	2.52
U(1)−B(6)	2.935(6)	U(1)−H(5E)	2.48
U(1)−H(1D)	2.57	U(1)−H(6D)	2.48
U(1)−H(1E)	2.37	U(1)−H(6E)	2.60
U(1)−H(2D)	2.42	U(1)−H(6F)′	2.50
U(1)−H(2E)	2.53	U(1)−U(1)′	5.991(6)
Bond Angles (deg)			
B(1)−U(1)−B(2)	53.45(19)	B(1)−U(1)−B(6)	108.31(19)
B(3)−U(1)−B(4)	53.05(18)	B(2)−U(1)−B(3)	111.2(2)
B(5)−U(1)−B(6)	51.86(17)	B(2)−U(1)−B(4)	93.5(2)
B(1)−N(1)−B(2)	109.4(4)	B(2)−U(1)−B(5)	141.91(19)
B(3)−N(2)−B(4)	109.8(4)	B(2)−U(1)−B(6)	93.56(17)
B(5)−N(3)−B(6)	108.8(4)	B(3)−U(1)−B(5)	106.51(19)
B(1)−U(1)−B(3)	110.90(19)	B(3)−U(1)−B(6)	140.74(18)
B(1)−U(1)−B(4)	138.2(2)	B(4)−U(1)−B(5)	105.1(2)
B(1)−U(1)−B(5)	116.7(2)	B(4)−U(1)−B(6)	97.15(18)

[a] Symmetry transformations used to generate equivalent atoms: ′ = x, −y+1/2, z−1/2.

$Na(H_3BNMe_2BH_3)$ in Et_2O. Cooling the resulting red toluene extracts afforded crystals of analytically pure $U(H_3BNMe_2BH_3)_3$ in much higher yield than when pentane was the extractant. The crystals do not contain toluene or diethyl ether and thus have the same composition as **1a**. Surprisingly, however, the crystals are red rather than brown. A crystallographic study revealed that the red crystals consist of a structural isomer of $U(H_3BNMe_2BH_3)_3$, which we will refer to as **1b** (Scheme 1).

Of the three aminodiboranate ligands per uranium center in **1b**, two are chelating and the third is bridging (Figure 2; Table 3). The local connectivity of each bridging ligand is $U(\kappa^3\text{-}H_3BNMe_2BH_3\text{-}\kappa^3)U$; i.e., the BH_3 groups are bound to different uranium centers, each in a κ^3 fashion. Thus, the uranium centers are again linked into a chain, but the chemical interactions responsible for

Scheme 1. Reaction Scheme and Reported Structures for the Uranium Aminodiboranates

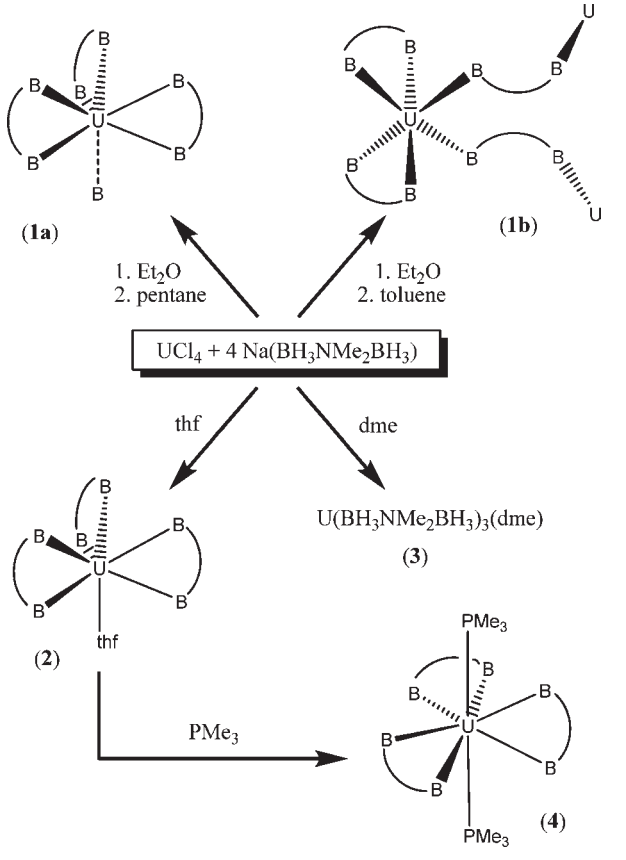

the polymeric structure are different in **1a** and **1b**. Each uranium center in **1b** is bound to two chelating ligands (forming eight U−H bonds) and to two ends of two bridging ligands (forming six U−H bonds); the total coordination number is therefore 14 (vs 13 in **1a**). The chelating U···B distances in **1b** range from 2.861(7)−2.902(6) Å, whereas the bridging U···B distances of 2.665(6) and 2.670(6) Å are much shorter, because

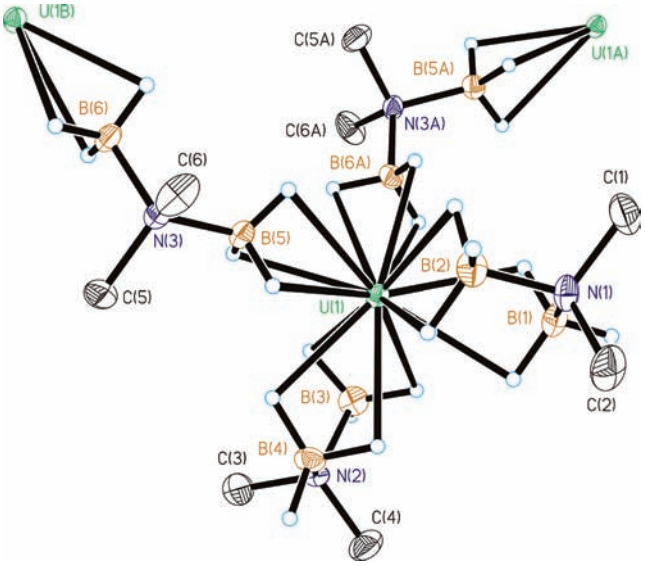

Figure 2. Molecular structure of $U(H_3BNMe_2BH_3)_3$, **1b**, obtained from toluene. Ellipsoids are drawn at the 35% probability level, except for hydrogen atoms, which are represented as arbitrarily sized spheres. The hydrogen atoms on the methyl groups have been removed for clarity.

Table 3. Selected Bond Lengths and Angles for $U(H_3BNMe_2BH_3)_3$, **1b**[a]

Bond Lengths (Å)			
U(1)−B(1)	2.902(6)	U(1)−H(22)	2.48(6)
U(1)−B(2)	2.862(7)	U(1)−H(31)	2.46(5)
U(1)−B(3)	2.861(7)	U(1)−H(32)	2.47(5)
U(1)−B(4)	2.889(6)	U(1)−H(41)	2.47(6)
U(1)−B(5)	2.670(6)	U(1)−H(42)	2.40(5)
U(1)−B(6)′	2.665(6)	U(1)−H(51)	2.31(5)
U(1)−H(11)	2.59(5)	U(1)−H(52)	2.51(5)
U(1)−H(12)	2.46(7)	U(1)−H(53)	2.46(5)
U(1)−H(21)	2.57(6)	U(1)−U(1)′	7.339(6)
Bond Angles (deg)			
B(1)−N(1)−B(2)	109.2(4)	B(2)−U(1)−B(4)	105.5(2)
B(3)−N(2)−B(4)	108.4(4)	B(2)−U(1)−B(5)	86.2(19)
B(5)−N(3)−B(6)	112.7(4)	B(2)−U(1)−B(6)′	113.2(2)
B(1)−U(1)−B(2)	53.16(18)	B(3)−U(1)−B(4)	53.0(2)
B(1)−U(1)−B(3)	100.2(2)	B(3)−U(1)−B(5)	118.3(2)
B(1)−U(1)−B(4)	104.0(2)	B(3)−U(1)−B(6)′	91.6(2)
B(1)−U(1)−B(5)	139.07(19)	B(4)−U(1)−B(5)	89.83(19)
B(1)−U(1)−B(6)′	96.70(19)	B(4)−U(1)−B(6)′	141.25(19)
B(2)−U(1)−B(3)	144.0(2)	B(5)−U(1)−B(6)′	95.59(19)

[a] Symmetry transformations used to generate equivalent atoms: ′ = $-x$, $y+1/2$, $-z+1/2$.

these contacts involve κ^3-BH_3 rather than κ^2-BH_3 interactions. The B−N−B angles in the chelating ligands of 108.4(4) and 109.2(4)° are similar to those observed in **1a**, but the B−N−B angles of 112.7(4)° in the bridging ligands are some 3° larger. The U···U distance between adjacent uranium centers in **1b** is 7.339(6) Å.

The different structural isomers seen for crystals grown from pentane and from toluene prompted us to examine whether the crystal structures were representative of the respective bulk samples. The dry solid obtained by evaporating a toluene solution of **1** gives a powder X-ray diffraction (XRD) pattern that matches that calculated from the single-crystal X-ray data collected for toluene-grown **1b**, even when the dried powder from toluene was thoroughly washed with pentane (Figure 3). In contrast, the XRD pattern of the powder obtained from the

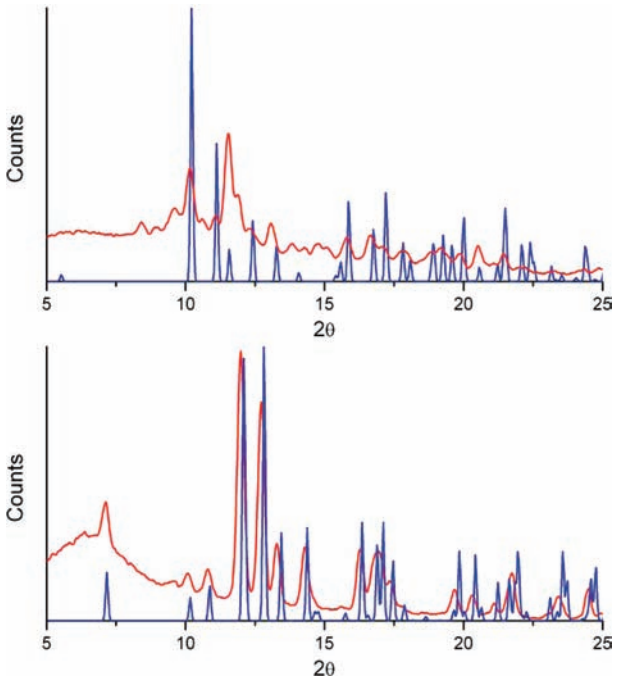

Figure 3. Analysis of extracts obtained from reactions to make $U(H_3BNMe_2BH_3)_3$ (see Experimental Section for details). Top: Experimental powder XRD pattern of solid obtained from pentane extract (red), and calculated powder XRD pattern from the single crystal diffraction data for **1a**. Bottom: Experimental powder XRD pattern of solid obtained from toluene extract (red), and calculated powder XRD pattern from the single crystal diffraction data for **1b** (blue).

pentane extract suggests that a mixture is present, of which **1a** (but not **1b**) is a component.

Structures analogous to those of **1a** and **1b** are also adopted by DMADB complexes of the larger (i.e., earlier) lanthanide ions.[20] Specifically, the 14-coordinate structure seen for **1b** is also adopted by the corresponding Pr^{3+} complex (r_{ionic} = 0.99 Å), whereas the 13-coordinate structure seen for **1a** is adopted by the DMADB complex of the smaller Sm^{3+} complex (r_{ionic} = 0.958 Å). The structural coexistence of both **1a** and **1b** implies that U^{3+} ought to be intermediate in size between Pr^{3+} and Sm^{3+}, but in fact it is larger than both (r_{ionic} = 1.025 Å).[24] The larger size of U^{3+} is also reflected in the average M···B distances to the chelating DMBDA ligands in the U, Pr, and Sm complexes, which are 2.920, 2.877, and 2.823 Å, respectively. Therefore, on the basis of the trends seen for the lanthanide complexes, U^{3+} should be too large to adopt a 13 coordinate structure but nevertheless, in structure **1a**, it does. The discrepancy may be ascribed to the usual explanation of unexpected features of the chemistry of uranium versus the lanthanides: the increased covalency of the uranium-ligand interactions.[25]

(24) Shannon, R. D. *Acta Crystallogr., Sect. A* **1976**, *A32*, 751–767.
(25) For some recent examples, including experimental and computational comparisons of metal−ligand covalency in trivalent lanthanide and actinide borohydride complexes, see: Arliguie, T.; Belkhiri, L.; Bouaoud, S.-E.; Thuery, P.; Villiers, C.; Boucekkine, A.; Ephritikhine, M. *Inorg. Chem.* **2009**, *48*, 221–230. Roger, M.; Belkhiri, L.; Arliguie, T.; Thuery, P.; Boucekkine, A.; Ephritikhine, M. *Organometallics* **2008**, *27*, 33–42. Ingram, K. I. ; Tassell, M. J.; Gaunt, A. J.; Kaltsoyannis, N. *Inorg. Chem.* **2008**, *47*, 7824–7833. Gaunt, A. J.; Reilly, S. D.; Enriquez, A. E.; Scott, B. L.; Ibers, J. A.; Sekar, P.; Ingram, K. I. ; Kaltsoyannis, N.; Neu, M. P. *Inorg. Chem.* **2008**, *47*, 29–41. Guillaumont, D. *THEOCHEM* **2006**, *771*, 105–110. Gaunt, A. J.; Scott, B. L.; Neu, M. P. *Angew. Chem., Int. Ed.* **2006**, *45*, 1638–1641.

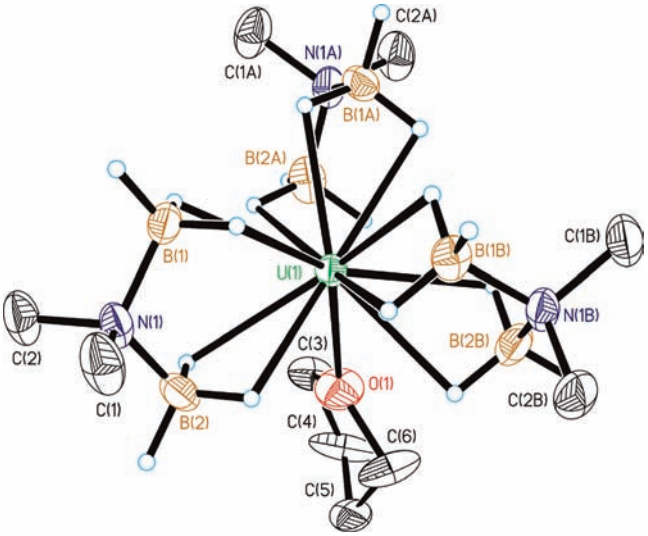

Figure 4. Molecular structure of $U(H_3BNMe_2BH_3)_3(thf)$, **2**. Ellipsoids are drawn at the 35% probability level, except for the hydrogen atoms, which are represented as arbitrarily sized spheres. Methyl and methylene hydrogen atoms have been deleted for clarity.

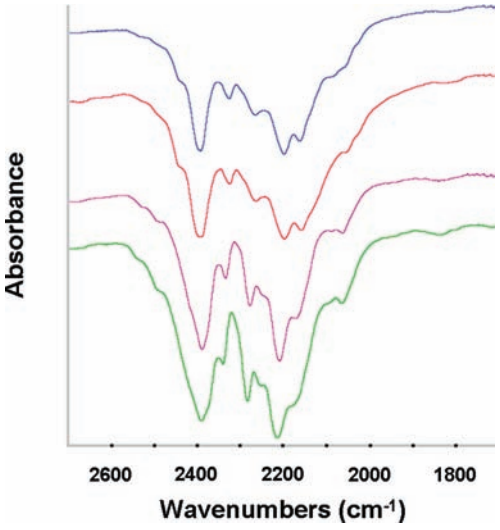

Figure 5. B−H stretching region in the IR spectrum (Nujol) of $U(H_3BNMe_2BH_3)_3$, **1a** (top, blue) and **1b** (red), $U(H_3BNMe_2BH_3)_3(thf)$, **2** (purple), and $Nd(H_3BNMe_2BH_3)_3(thf)$ (bottom, green) for comparison.

The IR spectra of solid samples of **1a** and **1b** are essentially identical, and feature a strong terminal B−H stretch at 2399 cm^{-1} and strong bridging B−H stretches at 2202 and 2168 cm^{-1} (Figure 5). Weaker B−H stretches are also observed at 2331 and 2270 cm^{-1}. When **1a** and **1b** are dissolved in toluene, they give identical ^1H NMR spectra: the NMe_2 groups appear as a paramagnetically shifted and broadened singlet at δ 3.76 (fwhm = 60 Hz), and the BH_3 groups appear as an even broader singlet at δ 91.3 (fwhm = 1100 Hz). The paramagnetism is due to the f^3 uranium(III) center, and the net effect on the NMR spectrum is very similar to that produced by the isoelectronic f^3 ion neodymium(III).[26] Thus, the ^1H NMR chemical shifts for **1a** and **1b** in toluene resemble those seen for $Nd(H_3BNMe_2BH_3)_3$ in benzene, which exhibits a NMe_2 signal at δ 4.66 (fwhm = 230 Hz) and a BH_3 signal at δ 86.8 (fwhm = 1400 Hz).[26] The ^{11}B NMR chemical shift of **1b** in toluene is δ 162.6, versus δ 125.3 for $Nd(H_3BNMe_2BH_3)_3$ in benzene.

Uranium(III) tris(tetrahydroborate) forms adducts of the form (η^6-arene)$U(BH_4)_3$,[27,28] but there is no evidence that **1** forms an analogous adduct with toluene in solution. Almost certainly, the increased steric bulk of DMADB versus BH_4^- leaves insufficient room for coordination of an η^6-arene ring to the uranium center.

Syntheses and Characterization of $U(H_3BNMe_2BH_3)_3$(thf) and $U(H_3BNMe_2BH_3)_3$(dme). The reaction of UCl_4 with 4 equiv of $Na(H_3BNMe_2BH_3)$ in tetrahydrofuran (thf) produces a green solution and some gas (probably H_2). Interestingly, the solution color does not change from green to brown, as seen in the analogous reaction in Et_2O. When the thf solvent is removed, however, the mixture slowly becomes dark brown, indicating reduction to U^{III}, if we assume that the green color attests to the presence of U^{IV}, as it does for $UCl_4(thf)_3$ and known U^{IV} borohydride complexes.[3,12,29−34] Extracting the dark residue with pentane and cooling the resulting extracts affords brown crystals of the new uranium(III) complex $U(H_3BNMe_2BH_3)_3(thf)$, **2**, which retains a coordinated tetrahydrofuran molecule.

Similarly, the reaction of UCl_4 with 4 equiv of $Na(H_3BNMe_2BH_3)$ in 1,2-dimethoxyethane (dme) also gives a solution that retains its original green color even after the mixture is stirred for several days. After evaporation of the solvent, the green residue slowly darkens under dynamic vacuum, and turns brown over the course of several hours. Extraction of the residue with benzene, followed by removal of the solvent, yields the new uranium(III) compound $U(H_3BNMe_2BH_3)_3(dme)$, **3**, but these samples proved to be somewhat impure. Fortunately, analytically pure samples can be prepared in good yield by adding dme to a solution of the thf adduct **2** in pentane, from which **3** can be obtained as a brown powder.

Crystals of the thf adduct **2** are isomorphous with those of the corresponding lanthanum compound $La(H_3BNMe_2BH_3)_3(thf)$,[26,35] both crystallizing in the cubic space group $I23$. The six boron atoms of the anions and the oxygen atom of the thf molecule describe a coordination polyhedron that is intermediate between a capped trigonal prism and a capped octahedron (Figure 4; Table 4). The U−O bond distance is 2.549(4) Å, and the U···B bond distances of 2.895(3) to 2.901(3) Å are comparable to those seen in **1a** and **1b**. The U−H distances range from

(26) Daly, S. R.; Kim, D. Y.; Girolami, G. S., manuscript in preparation.
(27) Baudry, D.; Bulot, E.; Ephritikhine, M. *J. Chem. Soc., Chem. Commun.* **1988**, 1369–1370.
(28) Baudry, D.; Bulot, E.; Charpin, P.; Ephritikhine, M.; Lance, M.; Nierlich, M.; Vigner, J. *J. Organomet. Chem.* **1989**, *371*, 155–162.
(29) Van Der Sluys, W. G.; Berg, J. M.; Barnhardt, D.; Sauer, N. N. *Inorg. Chim. Acta* **1993**, *204*, 251–256.
(30) Rietz, R. R.; Edelstein, N. M.; Ruben, H. W.; Templeton, D. H.; Zalkin, A. *Inorg. Chem.* **1978**, *17*, 658–660.
(31) Rietz, R. R.; Zalkin, A.; Templeton, D. H.; Edelstein, N. M.; Templeton, L. K. *Inorg. Chem.* **1978**, *17*, 653–658.
(32) Zalkin, A.; Rietz, R. R.; Templeton, D. H.; Edelstein, N. M. *Inorg. Chem.* **1978**, *17*, 661–663.
(33) Shinomoto, R.; Zalkin, A.; Edelstein, N. M. *Inorg. Chim. Acta* **1987**, *139*, 91–95.
(34) Shinomoto, R.; Zalkin, A.; Edelstein, N. M.; Zhang, D. *Inorg. Chem.* **1987**, *26*, 2868–2872.
(35) Girolami, G. S.; Kim, D. Y.; Abelson, J. R.; Kumar, N.; Yang, Y.; Daly, S. U.S. Patent Appl. 59728, April 9, 2008.

Table 4. Selected Bond Lengths and Angles for $U(H_3BNMe_2BH_3)_3(thf)$, **2**[a]

Bond Lengths (Å)			
U(1)−O(1)	2.549(4)	U(1)−H(1B)	2.4465
U(1)−B(1)	2.895(3)	U(1)−H(2A)	2.4621
U(1)−B(2)	2.901(3)	U(1)−H(2B)	2.5474
U(1)−H(1A)	2.5557		
Bond Angles (deg)			
H(1A)−U(1)−H(1B)	44.0(1)	B(2)−U(1)−B(1′)	104.2(1)
H(2A)−U(1)−H(2B)	44.0(1)	B(2)−U(1)−B(2″)	115.41(6)
B(1)−U(1)−B(2)	52.3(1)	B(1)−U(1)−O(1)	125.63(8)
B(1)−U(1)−B(1′)	89.49(11)	B(2)−U(1)−O(1)	77.44(9)
B(1)−U(1)−B(2′)	138.31(10)	B(1)−N(1)−B(2)	108.9(2)

[a] Symmetry transformations used to generate equivalent atoms: ′ = $-y+1, z, -x+1$ ″ = $-z+1, -x+1, y$.

2.45 to 2.56 Å, and the average B−N−B angle of the aminodiboranate ligands is 108.9(2)°, which is also very similar to the average angle seen in **1a**.

The IR spectrum of **2** in the B−H stretching region is similar to those observed for **1a** and **1b** and closely matches the spectrum of the neodymium analogue $Nd(H_3BNMe_2BH_3)_3(thf)$ (Figure 5). In addition, two IR peaks at 856 and 837 cm^{-1}, which are not present in the IR spectra of **1a** and **1b**, correspond to the symmetric C−O−C stretches of the coordinated thf molecule.[36,37] The asymmetric C−O−C stretches are masked by other peaks in the spectra. The field ionization mass spectrum of **2** shows peaks at $m/e = 72$ and 453 assignable to thf^+ and the ion $U(H_3BNMe_2BH_3)_3^+$, respectively.

The ^1H NMR chemical shifts of **2** are very similar to those observed for the analogous lanthanide complex $Nd(H_3BNMe_2BH_3)_3(thf)$, which also has an f^3 electronic configuration.[26,35] Thus, the chemical shifts of the NMe_2 and BH_3 protons in **2** are δ 3.36 and 104.4, respectively (vs δ 3.06 and 82.9 for the Nd analogue), and the α and β methylene protons of the thf ligand appear at δ −5.56 and −1.89 (vs δ 0.66 and 0.95 for the Nd analogue). The ^{11}B NMR chemical shift of **2** is δ 152.8, versus δ 104.8 for $Nd(H_3BNMe_2BH_3)_3(thf)$. Although the chemical shifts of the U and Nd complexes are not identical, they are remarkably similar in view of the large paramagnetic shielding and deshielding effects that are characteristic of U^{III} borohydride species.[38,39]

The ^1H and ^{11}B NMR spectra of the dme complex **3** are similar to those of **2** except for the resonances due to the coordinated dme. The IR spectrum of **3** exhibits a strong terminal B−H stretch at 2385 cm^{-1} and two strong bridging B−H stretches at 2290 and 2227 cm^{-1}; weaker B−H stretches are also observed at 2341 and 2173 cm^{-1}. Three peaks at 1089, 975, and 858 cm^{-1}, which are not present in the IR spectra of **1a** and **1b**, correspond to stretching vibrations of the coordinated dme molecule.[37]

Synthesis and Characterization of $U(H_3BNMe_2BH_3)_3(PMe_3)_2$. Addition of trimethylphosphine, PMe_3, to the thf adduct **2** in pentane affords a dark red solution, from which dark-red needles of the bis(trimethylphosphine) adduct $U(H_3BNMe_2BH_3)_3(PMe_3)_2$ (**4**) can be isolated. The crystal structure of **4** confirms that the uranium centers are bound to three chelating aminodiboranate ligands and to two PMe_3 ligands. The six boron atoms and two phosphorus atoms describe an approximate trigonal dodecahedron (Figure 6; Table 5), with atoms P1, P2, B1, and B2 forming one of the two interpenetrating trapezoids, and atoms B3, B4, B5, and B6 forming the second. The two PMe_3 ligands occupy the wingtip positions of one of the two trapezoids, so that the P−U−P angle is 168.92(2)°. The U···B distances range from 2.939(4) to 2.957(3) Å, and are slightly longer than those observed in **1a**, **1b**, and **2**. The U−P bond lengths of 3.1093(9) and 3.1145(8) Å are in good

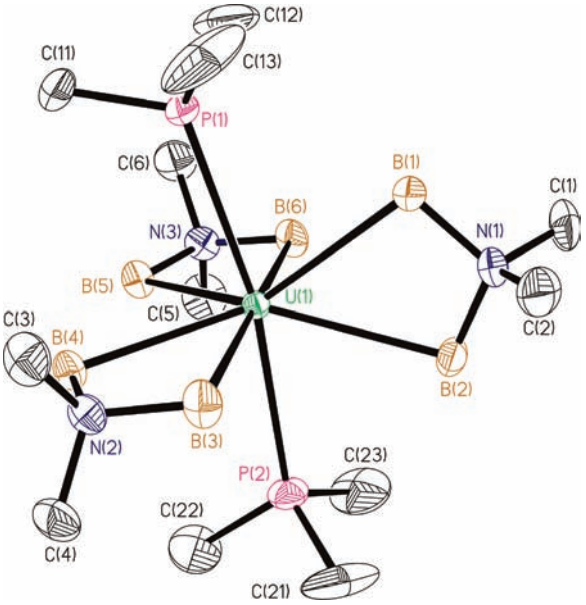

Figure 6. Molecular structure of $U(H_3BNMe_2BH_3)_3(PMe_3)_2$, **4**. Ellipsoids are drawn at the 35% probability level. Hydrogen atoms have been deleted for clarity.

Table 5. Selected Bond Lengths and Angles for $U(H_3BNMe_2BH_3)_3(PMe_3)_2$, **4**

Bond Lengths (Å)			
U(1)−B(1)	2.953(4)	U(1)−B(5)	2.944(3)
U(1)−B(2)	2.957(3)	U(1)−B(6)	2.949(4)
U(1)−B(3)	2.939(4)	U(1)−P(1)	3.114(1)
U(1)−B(4)	2.943(3)	U(1)−P(2)	3.109(1)
Bond Angles (deg)			
B(1)−U(1)−B(2)	51.21(9)	B(3)−U(1)−B(6)	173.10(11)
B(3)−U(1)−B(4)	50.88(9)	B(3)−U(1)−P(1)	93.75(9)
B(5)−U(1)−B(6)	50.90(9)	B(3)−U(1)−P(2)	86.45(9)
B(1)−U(1)−B(3)	93.07(11)	B(4)−U(1)−B(5)	74.05(9)
B(1)−U(1)−B(4)	133.41(11)	B(4)−U(1)−B(6)	124.94(9)
B(1)−U(1)−B(5)	135.46(10)	B(4)−U(1)−P(1)	83.31(8)
B(1)−U(1)−B(6)	93.31(11)	B(4)−U(1)−P(2)	88.27(8)
B(1)−U(1)−P(1)	69.12(7)	B(5)−U(1)−B(6)	50.90(9)
B(1)−U(1)−P(2)	121.95(7)	P(1)−U(1)−B(5)	84.16(7)
B(2)−U(1)−B(3)	90.08(11)	P(2)−U(1)−B(5)	86.61(7)
B(2)−U(1)−B(4)	137.39(10)	P(1)−U(1)−B(6)	90.97(8)
B(2)−U(1)−B(5)	137.68(10)	P(2)−U(1)−B(6)	87.95(8)
B(2)−U(1)−B(6)	91.87(10)	P(1)−U(1)−P(2)	168.92(2)
P(1)−U(1)−B(2)	120.33(7)	B(1)−N(1)−B(2)	108.4(2)
P(2)−U(1)−B(2)	70.74(7)	B(3)−N(2)−B(4)	107.1(2)
B(3)−U(1)−B(4)	50.88(9)	B(5)−N(3)−B(6)	107.9(2)
B(3)−U(1)−B(5)	124.62(10)		

(36) Clark, R. J. ; Lewis, J.; Machin, D. J.; Nyholm, R. S. *J. Chem. Soc.* **1963**, 379–387.
(37) Avens, L. R.; Bott, S. G.; Clark, D. L.; Sattelberger, A. P.; Watkin, J. G.; Zwick, B. D. *Inorg. Chem.* **1994**, *33*, 2248–2256.
(38) Fazakerley, G. V.; Folcher, G.; Marquet-Ellis, H. *Polyhedron* **1984**, *3*, 457–461.
(39) Ban, B.; Folcher, G.; Marquet-Ellis, H.; Rigny, P. *Nouv. J. Chim.* **1985**, *9*, 51–53.

agreement with U^{III} borohydride complexes containing the chelating phosphine 1,2-bis(dimethylphosphino)ethane (dmpe).[40,41]

Apart from **4**, there are only two other examples of structurally characterized uranium complexes with coordinated unidentate phosphines.[42,43] Usually, such species are unstable with respect to dissociation of the phosphine.[44] Uranium(III) borohydride complexes are known to be Lewis acidic; for example, $U(BH_4)_3$ strongly binds arene ligands.[27,28] Evidently, the uranium aminodiboranate complexes must also be reasonably Lewis acidic, so that binding of two PMe_3 ligands is strong.

The field ionization mass spectrum of **4** shows peaks corresponding to $U(H_3BNMe_2BH_3)_3^+$, $U(H_3BNMe_2BH_3)_3(PMe_3)^+$, and $U(H_3BNMe_2BH_3)_3(H_3BNMe_2BH_2PMe_3)^+$ at $m/z = 454$, 530, and 601, respectively. The ^1H NMR spectrum of **4** features a broadened singlet at δ −1.56 due to the PMe_3 groups and resonances at δ 4.03 and 98.3 due to the NMe_2 and BH_3 groups, respectively. The ^{11}B NMR chemical shift is δ 152.4. No signals were observed in the $^{31}P\{^1H\}$ NMR spectrum owing to the paramagnetism of the U^{III} center.

Magnetic Moments. The magnetic moments of **1**, **2**, and **4** at 293 K are 2.8, 2.9, and 2.7 μ_B, respectively. These values are similar to those of 2.59−2.92 μ_B at 300 K reported for certain U^{III} aryl-oxide complexes bearing functionalized triazacyclononane groups,[45−49] but are lower than the calculated μ_{eff} of 3.69 μ_B for a free U^{3+} ion.[50] Interestingly, some other U^{III} species such as $U_3(BH_4)_9$, $U(BH_4)_3$(2,2,2-cryptand), and $U[N(SiMe_3)_2]_3$ have magnetic moments of 3.1−3.4 μ_B that fall much closer to the free ion value.[23,51] It has been suggested that reduced magnetic moments can be attributed to a strong ligand field and, to a lesser extent, orbital reduction effects because of covalency in the metal ligand bonding.[48]

Reduction of U^{IV} to U^{III} by $Na(H_3BNMe_2BH_3)$. There are three notable aspects of the isolation of U^{III} products from the reaction of UCl_4 with $Na(H_3BNMe_2BH_3)$. First, the reductions are accompanied by the formation of a gas (undoubtedly H_2) and the organic byproduct (μ-dimethylamino)diborane, $(NMe_2)B_2H_5$; the latter was identified in the ^{11}B NMR spectra of the reaction solutions (see Experimental Section). Over the early stages of the reaction in thf, for every equivalent of $Na(H_3BNMe_2BH_3)$ consumed, 1 equiv of $(NMe_2)B_2H_5$ is generated, as shown by integrations relative to an internal ^{11}B NMR standard. Mass balance considerations suggest that the reaction of UCl_4 with $Na(H_3BNMe_2BH_3)$ initially generates $(NMe_2)B_2H_5$ and the uranium(IV) hydride, $UCl_3H(thf)_x$, and that the latter subsequently reductively eliminates H_2 and reduces to $UCl_3(thf)_x$. Similar mechanisms have been invoked in certain reductions of U^{IV} to U^{III} in the presence of BH_4,[39,40,51,52] and it is known that tetrahydroborate complexes of redox stable metal ions such as Zr^{4+} or Hf^{4+} can produce B_2H_6 and metal hydrides.[53−55] Evidently, relative to the reduction step, substitution of the remaining uranium-bound chloride ligands in $UCl_3(thf)_x$ with aminodiboranate anions in thf is slow, and in fact, the ^{11}B NMR studies suggest that these reactions take place only when the thf solvent is removed (see Supporting Information)

Second, the rate of reaction of UCl_4 with $Na(H_3BNMe_2BH_3)$ is solvent dependent, being slower in strongly coordinating ethers and faster in weakly coordinating ethers, as shown by time-dependent ^{11}B NMR studies of the UCl_4 + 4 $Na(H_3BNMe_2BH_3)$ reaction mixtures in Et_2O and thf. In Et_2O the resonance for $Na(H_3BNMe_2BH_3)$ disappears completely after 4 h of reaction time,[56] whereas in thf more than 85% of this starting material is still present after 22 h. A likely candidate for the solvent-dependent step is dissociation of solvent from the uranium center to create an open coordination site necessary for the substitution of a chloride ligand by an aminodiboranate anion. This dissociation will be slower for more strongly coordinating solvents.

Third, whereas the aminodiboranate ligand readily reduces U^{IV} to U^{III}, the analogous reactions of UCl_4 with $NaBH_4$ afford U^{IV} products at room temperature, with U^{III} products being generated only upon heating or by adding strong Lewis bases such as trialkylphosphines.[3,39,52,57] The different reducing power is consistent with the previous finding that organic substrates and transition metals are more readily reduced by $Na(H_3BNMe_2BH_3)$ than by $NaBH_4$.[17,35] We have carried out density functional theory (DFT) calculations to explore whether $Na(H_3BNMe_2BH_3)$ is in fact a stronger reductant than $NaBH_4$: the ionization energy of the BH_4^- anion (calculated from the energy difference between the BH_4^- anion and the BH_4 radical) is 90.6 kcal/mol, whereas the ionization energy of the $H_3BNMe_2BH_3^-$ 5anion is 86.1 kcal/mol. In other words, $H_3BNMe_2BH_3^-$ is a stronger reductant than BH_4^- by 4.5 kcal/mol, or 0.2 V.

It is important to consider, however, that the reduction of U^{IV} to U^{III} in this system is not a simple electron transfer but instead involves breaking B−H (and possibly U−H) bonds, and that these chemical steps are very likely

(40) Brennan, J.; Shinomoto, R.; Zalkin, A.; Edelstein, N. *Inorg. Chem.* **1984**, *23*, 4143–4146.
(41) Wasserman, H. J.; Moody, D. C.; Ryan, R. R. *J. Chem. Soc., Chem. Commun.* **1984**, 532–533.
(42) Brennan, J. G.; Zalkin, A. *Acta Crystallogr., Sect. C: Cryst. Struct. Commun.* **1985**, *41*, 1038–1040.
(43) Hayton, T. W.; Boncella, J. M.; Scott, B. L.; Batista, E. R.; Hay, P. J. *J. Am. Chem. Soc.* **2006**, *128*, 10549–10559.
(44) Manriquez, J. M.; Fagan, P. J.; Marks, T. J.; Vollmer, S. H.; Day, C. S.; Day, V. W. *J. Am. Chem. Soc.* **1979**, *101*, 5075–5078.
(45) Castro-Rodriguez, I.; Olsen, K.; Gantzel, P.; Meyer, K. *Chem. Commun.* **2002**, 2764–2765.
(46) Castro-Rodriguez, I.; Nakai, H.; Zakharov, L. N.; Rheingold, A. L.; Meyer, K. *Science* **2004**, *305*, 1757–1759.
(47) Nakai, H.; Hu, X.; Zakharov, L. N.; Rheingold, A. L.; Meyer, K. *Inorg. Chem.* **2004**, *43*, 855–857.
(48) Castro-Rodriguez, I.; Meyer, K. *Chem. Commun.* **2006**, 1353–1368.
(49) Lam, O. P.; Feng, P. L.; Heinemann, F. W.; O'Connor, J. M.; Meyer, K. *J. Am. Chem. Soc.* **2008**, *130*, 2806–2816.
(50) Jones, E. R., Jr.; Hendricks, M. E.; Stone, J. A.; Karraker, D. G. *J. Chem. Phys.* **1974**, *60*, 2088–2094.
(51) Dejean-Meyer, A.; Folcher, G.; Marquet-Ellis, H. *J. Chim. Phys. Phys.-Chim. Biol.* **1983**, *80*, 579–581.
(52) Baudry, D.; Charpin, P.; Ephritikhine, M.; Lance, M.; Nierlich, M.; Vigner, J. *J. Chem. Soc., Chem. Commun.* **1987**, 739–740.
(53) Marks, T. J.; Kolb, J. R. *Chem. Rev.* **1977**, *77*, 263–293.
(54) Gozum, J. E.; Girolami, G. S. *J. Am. Chem. Soc.* **1991**, *113*, 3829–3837.
(55) Gozum, J. E.; Wilson, S. R.; Girolami, G. S. *J. Am. Chem. Soc.* **1992**, *114*, 9483–9492.
(56) The decrease in the $Na(H_3BNMe_2BH_3)$ concentration is not due to precipitation because this salt is highly soluble in diethyl ether.
(57) Ghiassee, N.; Clay, P. G.; Walton, G. N. *J. Inorg. Nucl. Chem.* **1981**, *43*, 2909–2913.

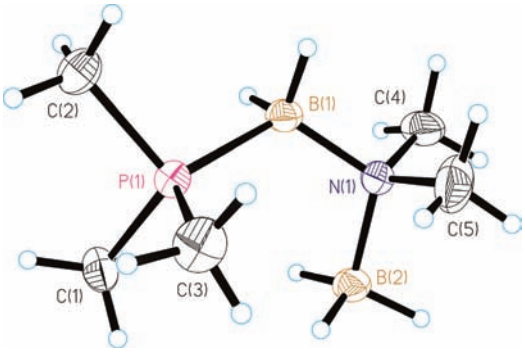

Figure 7. Molecular structure of $PMe_3BH_2NMe_2BH_3$, **5**. Ellipsoids are drawn at the 35% probability level, except for the hydrogen atoms, which are represented as arbitrarily sized spheres.

irreversible and could drive an otherwise electrochemically unfavorable redox reaction.[53] The fact that the reduction of UCl_4 by $Na(H_3BNMe_2BH_3)$ is faster in some solvents than in others strongly suggests that kinetic factors control the reduction process. All in all, however, the evidence at present does not allow us to distinguish between the following two explanations of why $H_3BNMe_2BH_3^-$ but not BH_4^- reduces U^{IV} to U^{III} at room temperature: $H_3BNMe_2BH_3^-$ is a stronger reductant than BH_4^- (a thermodynamic effect), or the barriers for the chemical processes associated with cleavage of B−H (and possibly U−H) bonds are larger for $H_3BNMe_2BH_3^-$ than for BH_4^- (a kinetic effect).

Chemical and Physical Properties of $U(H_3BNMe_2BH_3)_3$ Complexes and Characterization of $PMe_3BH_2NMe_2BH_3$. Complexes **1a**, **1b**, **2**, and **4** are air-sensitive (**1a** and **1b** especially so) and react vigorously with protic solvents such as alcohols and with halogenated solvents such as chloroform and dichloromethane. Addition of these solvents results in the evolution of gas and an immediate color change from brown to yellow. Similar reactivity has been observed for other U^{III} borohydride complexes.[58]

Compounds **1a**, **1b**, and **2** are thermally stable at room temperature for months when stored in sealed glassware under argon. In contrast, the PMe_3 adduct **4** slowly decomposes with loss of the phosphine-borane $PMe_3BH_2NMe_2BH_3$, **5**. This previously unreported compound has been characterized by its ^1H, ^{11}B, and $^{31}P\{^1H\}$ NMR spectra. The structure of **5** was also confirmed by single crystal X-ray diffraction of crystals grown from pentane (Figure 7; Table 6).

Our original interest in these uranium aminodiboranate complexes was to determine whether they were volatile and thus useful in chemical vapor deposition (CVD) processes. The uranium complexes $U(H_3BNMe_2BH_3)_3$, **1**, and $U(H_3BNMe_2BH_3)_3(thf)$, **2**, are direct analogues of lanthanide complexes that we have already investigated as CVD precursors.[20] Heating the thf adducts $Ln(H_3BNMe_2BH_3)_3(thf)$ in vacuum causes loss of thf and formation of the base-free species $Ln(H_3BNMe_2BH_3)_3$. The latter are highly volatile, and sublime in vacuum at temperatures as low as 65 °C without decomposition.[20] The uranium complexes have structures that are essentially identical to those seen for the early lanthanides, and so we expected their volatilities to be similar.

Table 6. Selected Bond Lengths and Angles for $PMe_3BH_2NMe_2BH_3$, **5**

Bond Lengths (Å)			
P(1)−B(1)	1.948(3)	B(1)−H(12)	1.074(16)
N(1)−B(1)	1.551(3)	B(2)−H(21)	1.126(13)
N(1)−B(2)	1.604(3)	B(2)−H(22)	1.136(14)
B(1)−H(11)	1.077(16)	B(2)−H(23)	1.123(13)
Bond Angles (deg)			
C(1)−P(1)−B(1)	117.02(12)	C(5)−N(1)−B(1)	111.09(18)
C(2)−P(1)−B(1)	105.22(13)	C(4)−N(1)−B(2)	108.12(18)
C(3)−P(1)−B(1)	118.24(13)	C(5)−N(1)−B(2)	108.5(2)
N(1)−B(1)−P(1)	118.48(17)	B(1)−N(1)−B(2)	113.38(17)
C(4)−N(1)−C(5)	108.3(2)	H(21)−B(2)−H(22)	110.9(16)
C(4)−N(1)−B(1)	107.3(2)		

To our surprise, attempts to sublime $U(H_3BNMe_2BH_3)_3(thf)$, **2**, at 10^{-2} Torr resulted instead in thermal decomposition, which afforded a metallic-appearing film on the surface of the glassware; similar behavior has been noted for $U(BH_4)_3(thf)_x$.[59] These results suggest that the uranium complexes decompose more rapidly than they sublime. The higher covalency of the U−H bond may mean that the B−H bonds in the uranium complexes are more readily cleaved than they are in the analogous lanthanide species. Efforts to discover new volatile uranium complexes continue.

Experimental Section

All operations were carried out in vacuum or under argon using standard Schlenk techniques. All glassware was dried in an oven at 150 °C, assembled hot, and allowed to cool under vacuum before use. Tetrahydrofuran, diethyl ether, and pentane were distilled under nitrogen from sodium/benzophenone and degassed with argon immediately before use. Toluene was dried similarly over molten sodium. The compounds UCl_4,[60] PMe_3,[61] and $Na(H_3BNMe_2BH_3)$[17] were prepared by literature routes.

Elemental analyses were carried out by the University of Illinois Microanalytical Laboratory. The IR spectra were recorded on a Nicolet Impact 410 infrared spectrometer as Nujol mulls between KBr plates. The ^1H data were obtained on a Varian Unity 400 instrument at 400 MHz or on a Varian Unity U500 instrument at 500 MHz. The ^{11}B NMR data were collected on a General Electric GN300WB instrument at 96 MHz or on a Varian Unity Inova 600 instrument at 192 MHz. Chemical shifts are reported in δ units (positive shifts to high frequency) relative to TMS (^1H) or $BF_3\cdot Et_2O$ (^{11}B). Field ionization (FI) mass spectra were recorded on a Micromass 70-VSE mass spectrometer. The shapes of all peak envelopes correspond with those calculated from the natural abundance isotopic distributions. Magnetic moments were determined in C_6D_6 by the Evans NMR method[62] on a Varian Gemini 500 instrument at 499.716 MHz. Melting points and decomposition temperatures were determined in closed capillaries under argon on a Thomas-Hoover Unimelt apparatus. Powder X-ray diffraction measurements were carried out on a Bruker P4RA/GADDS wide angle diffractometer using a Cu Kα radiation source.

Caution! *Uranium salts are alpha emitters and are known nephrotoxins. Inhalation should be avoided by conducting all*

(58) Dejean, A.; Charpin, P.; Folcher, G.; Rigny, P.; Navaza, A.; Tsoucaris, G. *Polyhedron* **1987**, *6*, 189–195.

(59) Moody, D. C.; Odom, J. D. *J. Inorg. Nucl. Chem.* **1979**, *41*, 533–535.
(60) Hermann, J. A.; Suttle, J. F. *Inorg. Synth.* **1957**, *5*, 143–145.
(61) Luetkens, M. L., Jr.; Sattelberger, A. P.; Murray, H. H.; Basil, J. D.; Fackler, J. P., Jr. *Inorg. Synth.* **1990**, *28*, 305–310.
(62) Sur, S. K. *J. Magn. Reson.* **1989**, *82*, 169–173.

*operations of dry materials in an approved fume hood and with proper safety equipment. Complexes **1a** and **1b** enflame upon exposure to air.*

Tris(*N*,*N*-dimethylaminodiboranato)uranium(III), U($H_3BNMe_2BH_3$)$_3$, Structural Isomer 1a. To a suspension of UCl_4 (0.27 g, 0.71 mmol) in diethyl ether (20 mL) at 0 °C was added a solution of sodium *N*,*N*-dimethylaminodiboranate (0.27 g, 2.9 mmol) in diethyl ether (20 mL). The mixture was warmed to room temperature and stirred for 17 h. Gas slowly evolved, and the bright green solution gradually turned dark brown over several hours. The brown mixture was evaporated to dryness under vacuum, and the brown residue was extracted with pentane (6 × 50 mL). The light brown extracts were combined, concentrated to 45 mL, and cooled to −20 °C to yield light brown crystals. Yield: 30 mg (9%). NMR and IR data were identical to those for isomer **1b**.

Structural Isomer 1b. To a suspension of UCl_4 (0.50 g, 1.3 mmol) in diethyl ether (15 mL) at 0 °C was added a solution of sodium *N*,*N*-dimethylaminodiboranate (0.51 g, 5.4 mmol) in diethyl ether (15 mL). The mixture was warmed to room temperature and stirred for 13 h. Gas slowly evolved, and the bright green solution gradually turned dark brown over several hours. The brown mixture was evaporated to dryness under vacuum, and the brown residue was extracted with toluene (2 × 25 mL). The red extracts were combined and evaporated to dryness under vacuum to yield a dark reddish-brown residue. The residue was washed with pentane (10 mL) and evaporated to dryness under vacuum to yield a dark orange powder. Yield: 0.32 g (53%). In another reaction, the residue was extracted with toluene (2 × 25 mL), concentrated to about 20 mL, and cooled to −20 °C to yield red microcrystals. Yield: 0.14 g, (26%). Mp 156 °C (dec). Anal. Calcd for $C_6H_{36}B_6N_3U$: C, 15.9; H, 8.01; N, 9.27. Found: C, 15.7; H, 7.50; N, 9.06. ^{1}H NMR (C_7D_8, 20 °C): δ 3.76 (br s, fwhm = 60 Hz, NMe_2, 36 H), 91.3 (br s, fwhm = 1100 Hz, BH_3). ^{11}B NMR (C_7D_8, 20 °C): δ 163.4 (br s, fwhm = 510 Hz). Magnetic moment (C_6D_6, 20 °C): 2.8 μ_B. IR (cm^{-1}): 2399 vs, 2331 m, 2270 s, 2202 vs, 2168 s, 2094 sh, 1402 w, 1327 sh, 1265 s, 1238 s, 1215 s, 1182 m, 1166 s, 1161 s, 1132 m, 1032 m, 928 m, 902 w, 808 w, 760 w, 451 m.

Tris(*N*,*N*-dimethylaminodiboranato)(tetrahydrofuran)uranium(III), U($H_3BNMe_2BH_3$)$_3$(thf), 2. To a suspension of UCl_4 (0.52 g, 1.4 mmol) in tetrahydrofuran (20 mL) at 0 °C was added a solution of sodium *N*,*N*-dimethylaminodiboranate (0.52 g, 5.5 mmol) in tetrahydrofuran (20 mL). The reaction mixture was warmed to room temperature, and a small amount of gas initially evolved. The mixture was stirred for 14 h to generate a green solution and a small amount of white precipitate. The mixture was evaporated to dryness under vacuum to afford a sticky dark brown solid, which was extracted with pentane (3 × 20 mL). The filtered extracts were combined, concentrated to about 28 mL, and cooled to −20 °C to yield 0.24 g of brown cubes. The mother liquor was concentrated to about 11 mL and cooled to −20 °C to yield an additional 0.14 g of product. Yield: 0.38 g (53%). Mp 135−136 °C. Anal. Calcd for $C_{10}H_{44}B_6N_3OU$: C, 22.9; H, 8.44; N, 7.99. Found: C, 22.8; H, 8.25; N, 7.66. ^{1}H NMR (C_6D_6, 20 °C): δ −5.56 (br s, fwhm = 125 Hz, α-thf, 4 H), −1.89 (br s, fwhm = 38 Hz, β-thf, 4 H), 3.36 (s, fwhm = 4 Hz, NMe_2, 18 H), 104.4 (br q, J_{BH} = 99 Hz, BH_3, 18 H). ^{11}B NMR (C_6D_6, 20 °C): δ 152.8 (br s, fwhm = 180 Hz). Magnetic moment (C_6D_6, 20 °C): 2.9 μ_B. MS(FI) [fragment ion, relative abundance]: *m*/*z* 453 [U($H_3BNMe_2BH_3$)$_3$, 15], 72 [thf, 100]. IR (cm^{-1}): 2390 vs, 2335 m, 2278 s, 2210 vs, 2173 sh, 2064 sh, 1400 w, 1236 s, 1217 s, 1186 s, 1169 s, 1136 s, 930 m, 903 w, 856 m, 837 m, 812 w, 451 m.

Tris(*N*,*N*-dimethylaminodiboranato)(1,2-dimethoxyethane)uranium(III), U($H_3BNMe_2BH_3$)$_3$(dme), 3. Method A. To a suspension of UCl_4 (0.34 g, 0.90 mmol) in 1,2-dimethoxyethane (20 mL) at 0 °C was added a solution of sodium *N*,*N*-dimethylaminodiboranate (0.34 g, 3.6 mmol) in dme (20 mL). The reaction mixture was warmed to room temperature and stirred for 15 h to generate a green solution and a small amount of white precipitate. The mixture was evaporated to dryness under vacuum to afford a sticky dark green solid, which slowly turned brown under dynamic vacuum over several hours. The residue was extracted with benzene (2 × 25 mL), and the extracts were filtered, combined, and evaporated to dryness under vacuum. The evaporated residue was washed with pentane (2 × 10 mL) to yield a free-flowing, dark mustard colored powder. Yield: 0.20 g. The NMR spectra of this powder were identical to those seen for the material made by method B below, but the microanalytical data suggested that the powder contained an NMR-silent impurity. Anal. Calcd for $C_{10}H_{46}B_6N_3O_2U$: C, 22.1; H, 8.53; N, 7.73. Ranges found (four samples): C, 16.65−18.15; H, 6.44−7.27; N, 6.01−7.25.

Method B. To U($H_3BNMe_2BH_3$)$_3$(thf) (0.16 g, 0.30 mmol) in pentane (20 mL) was added 1,2-dimethoxyethane (0.5 mL). A small amount of precipitate immediately formed. The brown mixture was stirred for several hours and then filtered. The filtrate was taken to dryness under vacuum to afford a crystalline brown powder. Yield: 0.10 g (58%). Mp 138 °C (dec.). Anal. Calcd for $C_{10}H_{46}B_6N_3O_2U$: C, 22.1; H, 8.53; N, 7.73. Found: C, 22.2; H, 8.39; N, 7.40. ^{1}H NMR (C_6D_6, 600 MHz, 20 °C): δ −2.23 (br s, fwhm = 100 Hz, OCH_2, 4 H), 2.64 (s, fwhm = 25 Hz, NMe_2, 18 H), 3.25 (s, fwhm = 45 Hz, OMe, 6 H), 94.8 (br s, fwhm = 410 Hz, BH_3, 18 H). ^{11}B NMR (C_6D_6, 192 MHz, 20 °C): 152.6 (br s, fwhm = 230 Hz, BH_3). IR (cm^{-1}): 2385 vs, 2341 m, 2290 s, 2227 vs, 2173 sh, 2056 sh, 1260 s, 1236 s, 1215 m, 1185 m, 1166 s, 1137 s, 1129 sh, 1089 m, 1034 s, 1013 vs, 975 w, 926 w, 904 w, 858 s, 815 w, 724 s, 447 m.

Tris(*N*,*N*-dimethylaminodiboranato)bis(trimethylphosphine)uranium(III), U($H_3BNMe_2BH_3$)$_3$(PMe_3)$_2$, 4. To U($H_3BNMe_2BH_3$)$_3$(thf) (0.18 g, 0.34 mmol) in pentane (20 mL) was added trimethylphosphine (0.14 mL, 1.4 mmol). The brown solution immediately turned dark red. The solution was stirred for 20 min, concentrated to 10 mL, and cooled to −20 °C to yield dark red crystals. Yield: 0.13 g (64%). Mp 173 °C (dec). Anal. Calcd for $C_{12}H_{54}B_6N_3P_2U$: C, 23.8; H, 8.99; N, 6.94. Found: C, 23.7; H, 9.30; N, 6.80. ^{1}H NMR (C_6D_6, 20 °C): δ −1.56 (br s, fwhm = 110 Hz, PMe_3, 18 H), 4.03 (s, fwhm = 4 Hz, NMe_2, 36 H), 98.3 (br s, fwhm = 330 Hz, BH_3, 36 H). ^{11}B NMR (C_6D_6, 20 °C): δ 152.4 (br s, fwhm = 190 Hz). MS(FI) [fragment ion, relative abundance]: *m*/*z* 601 [U($H_3BNMe_2BH_3$)$_3$($H_3BNMe_2BH_2PMe_3$)$^+$, 75], 530 [U($H_3BNMe_2BH_3$)$_3$(PMe_3)$^+$, 100], 454 [U($H_3BNMe_2BH_3$)$_3^+$, 83]. Magnetic moment (C_6D_6, 20 °C): 2.7 μ_B. IR (cm^{-1}): 2379 vs, 2355 vs, 2329 m, 2269 m, 2207 vs, 2164 sh, 2061 w, 1303 w, 1284 w, 1228 s, 1213 m, 1182 sh, 1163 vs, 1136 s, 947 m, 923 sh, 904 sh, 812 w, 459 m.

μ-(*N*,*N*-Dimethylamido)pentahydro(trimethylphosphine)diboron, $PMe_3BH_2NMe_2BH_3$, 5. Method A. At room temperature under an inert atmosphere, crystals of **4** change color from dark red to grayish-black over several months (in contrast, crystals of **1a**, **1b**, and **2** are unchanged over these periods). Extraction of these aged crystals with C_6D_6 afforded a red solution and large amounts of an insoluble brown solid. The NMR spectra of the soluble fraction revealed the presence of **4** and the phosphinoborane $PMe_3BH_2NMe_2BH_3$, **5**, which had the following NMR parameters. ^{1}H NMR (C_6D_6, 20 °C): δ 0.78 (d, J_{PH} = 10 Hz, PMe_3, 9 H), 2.24 (q, J_{BH} = 102 Hz, BH_2, 2 H), 2.41 (q, J_{BH} = 93 Hz, BH_3, 3 H), 2.50 (s, NMe_2, 6 H). ^{11}B NMR (C_6D_6, 20 °C): δ −9.7 (td, J_{PB} = 81 Hz, J_{HB} = 102 Hz), −9.1 (q, J_{HB} = 95 Hz). ^{31}P{^{1}H} NMR (C_6D_6, 20 °C): −13.4 (q, J_{BP} = 76 Hz).

Method B. To a suspension of UCl_4 (0.25 g, 0.66 mmol) in thf (10 mL) was added sodium *N*,*N*-dimethylaminodiboranate (0.25 g, 2.6 mmol) in Et_2O (10 mL). The reaction mixture was warmed to room temperature and a small amount of gas initially evolved. The mixture stirred for 14 h to generate a green solution and a small amount of white precipitate. The mixture was evaporated to dryness under vacuum to afford a sticky dark brown solid, which was extracted with pentane (3 × 5 mL) and

filtered. To the filtered extract was added PMe_3 (0.21 mL, 2.0 mmol) via syringe. The brown solution immediately turned dark red. The red solution was filtered, concentrated to about 8 mL, and cooled to −20 °C. Colorless plates co-crystallized with red crystals of **4**. The NMR spectra showed that the colorless plates were the phosphinoborane **5**.

NMR Studies of the Reaction of UCl_4 with $Na(H_3BNMe_2BH_3)$. Aliquots of the UCl_4 + 4 $Na(H_3BNMe_2BH_3)$ reaction mixtures used to synthesize **1a**, **1b**, and **2** were taken periodically, and the aliquots were examined by ^{11}B NMR spectroscopy. Sealed capillaries containing a 0.7 M solution of $NaBPh_4$ in diglyme were used as an internal ^{11}B NMR standard. Further details of these NMR studies, including the detection of (μ-dimethylamino)diborane byproduct, $B_2H_5(NMe_2)$, can be found in the Supporting Information.

DFT Calculations. Calculations were performed with Gaussian03 Rev. C.02.[63] All structures were optimized with the B3LYP functional and the valence double-ζ polarized 6-31G* Pople basis set, which includes six d-type Cartesian-Gaussian polarization functions for the non-hydrogen atoms. Typical absolute errors in DFT calculations of ionization potentials are on the order of 0.2 eV,[64] but the relative error for similar molecules or ions should be smaller than this value.

Crystallographic Studies.[65] Single crystals obtained from pentane (**1a**, **2**, **4**, and **5**) or toluene (**1b**) were mounted on glass fibers with Paratone-N oil (Exxon) and immediately cooled to −80 °C in a cold nitrogen gas stream on the diffractometer. Standard peak search and indexing procedures, followed by least-squares refinement yielded the cell dimensions given in Table 1. The measured intensities were reduced to structure factor amplitudes and their estimated standard deviations by correction for background and Lorentz and polarization effects. No corrections for crystal decay were necessary but a face-indexed absorption correction was applied. Systematically absent reflections were deleted and symmetry equivalent reflections were averaged to yield the set of unique data. Except where noted, all unique data were used in the least-squares refinements. The analytical approximations to the scattering factors were used, and all structure factors were corrected for both real and imaginary components of anomalous dispersion. Correct atomic position(s) were deduced from an E-map (SHELX); least-squares refinement and difference Fourier calculations were used to locate atoms not found in the initial solution. Except where noted below, hydrogen atoms were placed in idealized positions with C−H (methyl) = 0.98 Å, C−H (methylene) = 0.99 Å, and B−H = 1.15 Å; idealized methyl and boranyl groups were allowed to rotate about their respective axes to find the best least-squares positions. In the final cycle of least-squares, independent anisotropic displacement factors were refined for the non-hydrogen atoms. The displacement parameters for methylene and boranyl hydrogens were set equal to 1.2 times U_{eq} for the attached carbon and boron, respectively; those for methyl hydrogens were set to 1.5 times U_{eq} for the attached carbon. No correction for isotropic extinction was necessary. Successful convergence was indicated by the maximum shift/error of 0.000 for the last cycle. A final analysis of variance between observed and calculated structure factors showed no apparent errors. Aspects of the refinements unique to each structure are reported below.

$U(H_3BNMe_2BH_3)_3$, 1a. The monoclinic lattice and systematic absences $0k0$ ($k \neq 2n$) and $h0l$ ($l \neq 2n$) were uniquely consistent with the space group $P2_1/c$, which was confirmed by the success of the subsequent refinement. The quantity minimized by the least-squares program was $\sum w(F_o^2 - F_c^2)^2$, where $w = \{[\sigma(F_o^2)]^2 + (0.0318P)^2\}^{-1}$ and $P = (F_o^2 + 2F_c^2)/3$. The largest peak in the final Fourier difference map (2.90 e Å^{-3}) was located 0.96 Å from U1.

$U(H_3BNMe_2BH_3)_3$, 1b. The monoclinic lattice and systematic absences $0k0$ ($k \neq 2n$) and $h0l$ ($l \neq 2n$) were uniquely consistent with the space group $P2_1/c$, which was confirmed by the success of the subsequent refinement. The quantity minimized by the least-squares program was $\sum w(F_o^2 - F_c^2)^2$, where $w = \{[\sigma(F_o^2)]^2 + (0.374P)^2\}^{-1}$ and $P = (F_o^2 + 2F_c^2)/3$. The boranyl hydrogen atoms were located in the difference maps, and their positions were refined with independent isotropic displacement parameters. Chemically equivalent B−H distances within the BH_3 units were constrained to be equal within a standard deviation of 0.01 Å. The remaining hydrogen atoms were placed in idealized positions. The largest peak in the final Fourier difference map (4.18 e Å^{-3}) was located 0.96 Å from U1.

$U(H_3BNMe_2BH_3)_3(thf)$, 2. The cubic $m\bar{3}$ Laue symmetry and systematic absences hkl ($h + k + l \neq 2n$) were consistent with space groups $Im\bar{3}$, $I23$, and $I2_13$; the noncentrosymmetric group $I23$ was shown to be the correct choice by successful refinement of the proposed model. The reflections 011 and 103 were statistical outliers and were deleted. The quantity minimized by the least-squares program was $\sum w(F_o^2 - F_c^2)^2$, where $w = \{[\sigma(F_o^2)]^2 + (0.0201P)^2\}^{-1}$ and $P = (F_o^2 + 2F_c^2)/3$. The tetrahydrofuran molecule was disordered about a 3-fold axis and its C−O and C−C bond distances were fixed at 1.48 ± 0.01 and 1.52 ± 0.01 Å, respectively. The largest peak in the final Fourier difference map (0.58 e Å^{-3}) was located 0.72 Å from U1.

$U(H_3BNMe_2BH_3)_3(PMe_3)_2$, 4. The orthorhombic lattice and the systematic absences $0kl$ ($k \neq 2n$), $h0l$ ($l \neq 2n$), and $hk0$ ($h \neq 2n$) were uniquely consistent with the space group *Pbca*, which was confirmed by the success of the subsequent refinement. The reflections 104, 202, 002, 106, and 102 were statistical outliers and were deleted. The quantity minimized by the least-squares program was $\sum w(F_o^2 - F_c^2)^2$, where $w = \{[\sigma(F_o^2)]^2 + (0.0238P)^2\}^{-1}$ and $P = (F_o^2 + 2F_c^2)/3$. The largest peak in the final Fourier difference map (0.75 e Å^{-3}) was located 1.01 Å from U1.

$PMe_3BH_2NMe_2BH_3$, 5. The orthorhombic lattice and the systematic absences $0kl$ ($l \neq 2n$) and $h0l$ ($h \neq 2n$) were consistent with the space groups $Pca2_1$ and *Pbcm*; the non-centrosymmetric space group $Pca2_1$ was shown to be the correct choice by successful refinement of the proposed model. The hydrogen atoms attached to boron were located in the difference maps, and their positions were refined with independent isotropic displacement parameters. Chemically equivalent B−H distances were constrained to be equal within a standard deviation of 0.01 Å. The remaining hydrogen atoms were placed in idealized positions. The quantity minimized by the least-squares program was $\sum w(F_o^2 - F_c^2)^2$, where $w = \{[\sigma(F_o^2)]^2 + (0.0398P)^2\}^{-1}$ and $P = (F_o^2 + 2F_c^2)/3$. The largest peak in the final Fourier difference map (0.20 e Å^{-3}) was located 0.92 Å from C2.

Acknowledgment. We thank the National Science Foundation (CHE07-50422 and DMR-0420768) and the PG Research Foundation for support of this research, and Scott Wilson and Teresa Wieckowska-Prussak for collecting the X-ray diffraction data. We also thank Charity Flener-Lovitt for performing the DFT calculations.

Supporting Information Available: X-ray crystallographic data (CIF format), and full description of the NMR studies of the reaction of UCl_4 with $Na(H_3BNMe_2BH_3)$ in Et_2O and thf. This material is available free of charge via the Internet at http://pubs.acs.org.

(63) Frisch, M. J.; et al. *Gaussian03*, Rev. C.02; Gaussian, Inc.: Wallingford, CT, 2004.

(64) Koch, W.; Holthause, M. C. *A Chemist's Guide to Density Functional Theory*, 2nd ed.; Wiley-VCH: Weinheim, 2002; Section 9.4.

(65) For details of the crystallographic methods used, see: Brumaghim, J. L.; Priepot, J. G.; Girolami, G. S. *Organometallics* **1999**, *18*, 2139–2144.